

## **Chapter 2 Soil Electromagnetic Properties and Applications in Geotechnical Engineering – A Review**

### **2.1 Introduction**

The potential usefulness of electromagnetic (EM) waves for soil physical and mechanical property characterization has long been recognized because of their nondestructive virtues. During the last several decades, many empirical correlations have been established to relate the EM properties of soils to their engineering properties. Some of these correlations are summarized in this chapter. Such a summary enables us to recognize the possibility of determining many soil engineering properties from the electromagnetic measurements, examine the validity of the established correlations, clarify the mechanisms underlying these correlations, and develop new and more reliable correlations.

To give a general impression on how different soils respond differently to an electromagnetic field and explain why they behave that way, the discussion starts with an introduction to soil electromagnetic properties and is followed by an explanation on why some soils exhibit a dielectric dispersion behavior in an electromagnetic field.

### **2.2 Soil Electromagnetic Properties**

The electromagnetic properties of a soil include its magnetic permeability, direct current (DC) electrical conductivity, and dielectric permittivity. Since most soils are non-ferromagnetic, soil electromagnetic properties usually only refer to their DC electrical conductivity and dielectric permittivity. The dielectric permittivity  $\epsilon$ , usually normalized

by the dielectric permittivity of vacuum  $\varepsilon_0$  [ $8.85 \times 10^{-12} \text{ C}^2 / (\text{Nm}^2)$ ], can be expressed as:

$$\kappa = \frac{\varepsilon}{\varepsilon_0} = \kappa' - j\kappa'' \quad [2.1]$$

where  $j = \sqrt{-1}$ . The real component  $\kappa'$  represents the polarization property of a soil. In engineering practice, it is frequently termed the *dielectric constant*. However,  $\kappa'$  is actually a frequency-dependent parameter. Therefore, it is named real permittivity in this study. The imaginary component  $\kappa''$  is usually termed the *polarization loss*, which represents the energy loss caused by a delay in the soil's responses to an applied field.

In addition to the polarization loss  $\kappa''$ , the DC electrical conductivity  $\sigma_{dc}$  also contributes to the energy loss. Thus, an effective electrical conductivity  $\sigma_{eff}$  is defined to account for the polarization loss at frequency  $f$  and the losses caused by the DC electrical conductivity:

$$\sigma_{eff} = 2\pi f \varepsilon_0 \cdot \kappa'' + \sigma_{dc} \quad [2.2]$$

The DC electrical conductivity provides a constant contribution to the effective electrical conductivity, while the contribution from the polarization loss is frequency-dependent. At low frequencies where the contribution of  $\kappa''$  is small,  $\sigma_{eff}$  can be approximated by the DC electrical conductivity  $\sigma_{dc}$ .

To characterize both the polarization property and energy losses of a material, an equivalent dielectric permittivity  $\kappa^*$  is defined by Ramo et al. (1994) as:

$$\kappa^* = \kappa' - j\left(\kappa'' + \frac{\sigma_{dc}}{2\pi f \varepsilon_0}\right) \quad [2.3]$$

in which, the imaginary permittivity  $\kappa'' + \frac{\sigma_{dc}}{2\pi f \epsilon_0}$  is obtained by dividing the effective electrical conductivity  $\sigma_{eff}$  by  $2\pi f \epsilon_0$ .

Plots of the real and imaginary permittivities as a function of frequency are called the frequency domain dielectric spectrum. Over the 1 MHz to 1 GHz frequency range, it was found that the real permittivity of a sand-water mixture does not change much with frequency, while the real permittivity of a clay-water mixture decreases with increasing frequency as shown in Figure 2.1, a phenomenon termed *dielectric dispersion*. Therefore, the real permittivity as a function of frequency is sometimes called the dielectric dispersion curve and the decrease of real permittivity over a certain frequency range, for example from 10 MHz to 1 GHz, is called the dielectric dispersion magnitude  $\Delta\kappa'$  over that frequency range. It was also observed that high specific surface area minerals usually exhibit higher dielectric dispersion magnitudes than low specific surface area minerals (Arulanandan 2003).

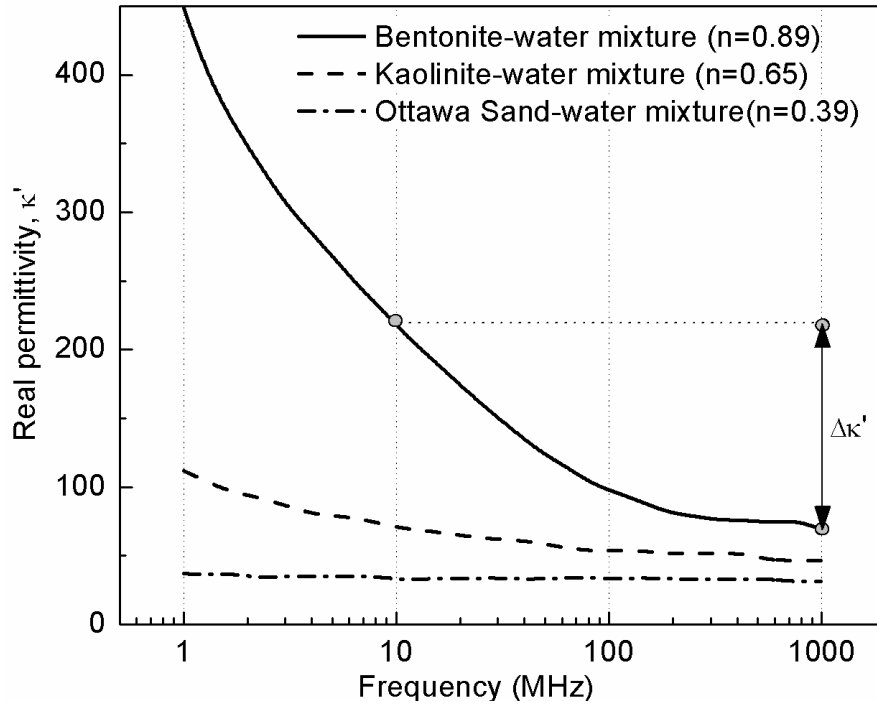


Figure 2.1 Typical dielectric dispersion curves of sand-water and clay-water mixtures (data from Rinaldi and Francisca, 1999) ( $n$  = porosity of the mixture,  $\Delta\kappa'$  = dielectric dispersion magnitude)

### 2.3 Important Polarization Mechanisms

Soil polarization characterized by the real permittivity  $k'$  arises from the displacement of charges from their equilibrium positions under the influence of an external EM field. Important polarization mechanisms include: electronic, ionic, orientational (dipolar molecules) polarization, interfacial polarization, counterion diffusion polarization, and electrode polarization. Predominant polarization mechanisms and the frequency ranges over which they are effective are shown in Figure 2.2. These important polarization mechanisms are also listed in Table 2.1. At increasing frequencies, some polarization mechanisms are no longer effective because of the decreasing ability of

the particles, molecules, ions, and internal structures to adjust to the rapidly reversing potential field. Thus, the real permittivity decreases with increase of frequency.

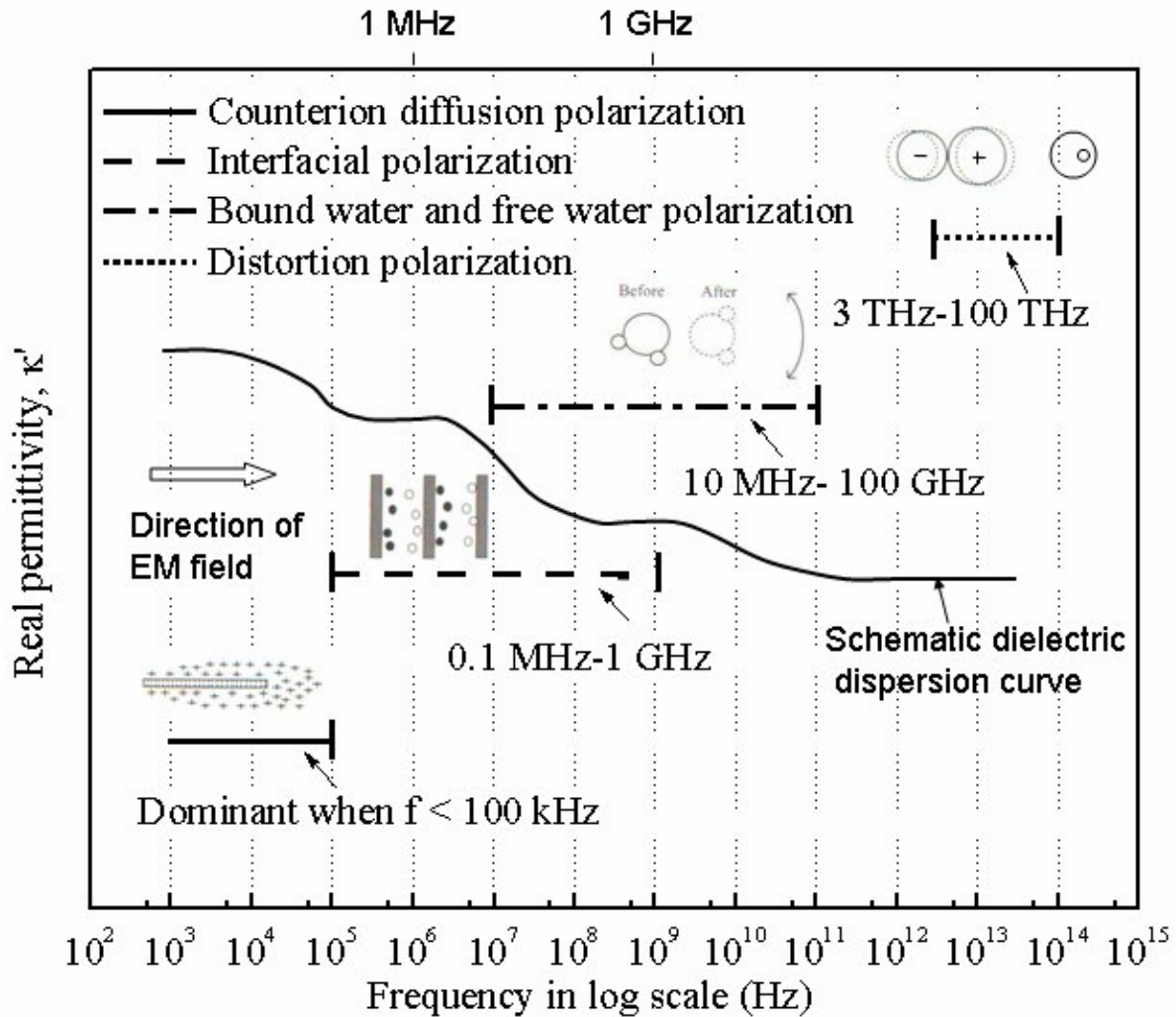


Figure 2.2 Effective frequency ranges of major polarization mechanisms

Table 2.1 Description of polarization mechanisms

Type	Counterion diffusion polarization	Interfacial polarization	Bound water and free water polarization	Distortion Polarization
Typical range	<100 kHz	0.1MHz-500MHz	10MHz-100GHz	3THz-100THz
Mechanisms	Polarization due to separation of cations and anions in the diffuse double layer	Results from alternately distributed conducting and non-conducting areas; not really a polarization phenomenon	Free water relaxation frequency is about 19 GHz. Bonds between the water molecules and soil particles lead to a lower relaxation frequency of bonded water than free water.	Displacement of electron clouds or a change of the distance between charged atoms (ions)
Current Use	Electrical mapping	Electrical capacitance probe	TDR, Ground penetrating radar	

Distortion polarization occurs at the atomic level. It is caused by a displacement of electron clouds against the nucleus or a change in distance between the charged atoms or ions. At frequencies less than 10 GHz, distortion polarization is independent of the frequency and temperature. In other words, the dielectric dispersion behavior at frequencies less than 10 GHz will not be affected by distortion polarization because distortion polarization provides a constant contribution to the real permittivity. More comprehensive treatment of distortion polarization is given by Santamarina et al. (2001).

Counterion diffusion polarization is caused by the separation of cations and anions in the diffuse double layer surrounding a clay plate in an EM field. It dominates at frequencies less than 0.1 MHz but may still contribute to the real permittivity  $\kappa'$  at frequencies higher than 1 MHz (Polk and Postow 1986). However, when soil particles are closely compacted, the counterion diffusion polarization will be hindered due to the ability of ions to move through adjacent neighboring double layers, which prevents the

distortion (displacement) of the double layer (Klein 1997). More discussion on the counterion diffusion polarization can be found in Hilhorst (1998).

Interfacial polarization, sometimes termed the Maxwell-Wagner effect, results from the alternate distribution of constituents with different electromagnetic properties in a soil. The potential difference acting across each constituent has to be different in order to maintain the same current density across different constituents, which is only possible when charges accumulate at the interfaces between soil constituents (Santamarina et al. 2001). The accumulation of electric charges at the interfaces enhances the polarizability of a soil and increases the real permittivity of the soil.

Water polarization results from the directional alignment of water molecules in an external EM field. In an alternating EM field, the rotation of the water molecules close to soil surfaces is hindered by surface forces arising from the solid-phase surface atoms. These water molecules are termed bound water molecules. Correspondingly, water molecules that are not subjected to soil surface forces are called free water molecules. The dielectric properties of bound water molecules are different from those of free water molecules (Hallikainen et al. 1985).

It can be seen from Figure 2.2 that the dielectric dispersion curve over the 1 MHz to 1 GHz frequency range is primarily affected by interfacial polarization and water polarization, and the effective frequency ranges of these two polarization mechanisms overlay with each other. The relative importance of each mechanism to the electromagnetic properties of a soil depends on the components and structure of a soil, which is discussed in the next chapter.

## 2.4 Current Applications

Electromagnetic property measurements have broad application in many branches of geoen지니어ing, for example, to monitor the transport of pollutants in the ground (e.g. Dahan et al. 2006; Sauck 2000), to characterize oil reservoirs in petroleum engineering (e.g. Prochnow et al. 2006) and to derive the engineering properties of geomaterials in geotechnical engineering (e.g. Arulanandan 2003). The soil engineering properties that can be determined by EM measurements are divided into four categories in the this summary: (1) water content and dry density from time domain reflectometry (TDR) measurements; (2) void ratio and anisotropy of granular soils from direct current electrical conductivity measurement. The correlations between the electrical conductivities and the small strain shear modulus, liquefaction potential and hydraulic conductivity belong to this category. (3) Specific surface area from thermal perturbation and dielectric dispersion. The determination of the critical state shear strength, compressibility and swelling potential from electromagnetic measurements belongs to this category. (4) Time-dependent soil behaviors. These applications are summarized in Table 2.2.



Table 2.2 Summary of the applications of electromagnetic measurements in geotechnical engineering

Properties	Measured Parameters	Frequency	References	Comments
Water content,	Apparent dielectric permittivity from TDR	about 1GHz	(Benson and Bosscher 1999; Noborio 2001; Topp et al. 1980)	Reliable method for many soils except for fat soils with high water content. Theory is sound. Experimental results support the theory. Correlations are strong.
Dry density	Combination of the apparent dielectric permittivity and bulk soil dc electrical conductivity	about 1GHz	(Yu and Drnevich 2004)	
Void ratio	Real permittivity	about 1GHz	(Dong and Wang 2005)	Theoretical mixing rule and empirical method are available to correlate void ratio to permittivity; no theory is universally applicable.
		50MHz	(Arulanandan 1991)	Theory based on Maxwell-Fricke electromagnetic theory is persuasive. Correlation for granular soils is strong. Applicability for clay needs further study
	Electrical conductivity	< 1 MHz	(Meegoda et al. 1989)	Correlation for granular soils is strong. Not applicable for clayey soils
Anisotropy	Directional electrical conductivity	< 1 MHz	(Meegoda et al. 1989)	Theory based on FEM analysis. Only applies for granular soil.
Stiffness	Electrical conductivity	< 1 MHz	(Arulanandan and Muraleetharan 1988; Arulmoli et al. 1985)	For granular soils only. Essentially demonstrate that the stiffness is closely related to the porosity and anisotropy
Liquefaction	Electrical conductivity	< 1 MHz	Same as above	Same as the correlation for stiffness

Table 2.2 Applications of electromagnetic measurements in geotechnical engineering (continued).

Properties	Measured Parameters	Frequency	References	Comments
Total specific surface area	Dielectric dispersion magnitude	1-150 MHz	(Meegoda 1985)	Experimental results are good but have some confusing points. No good theory. More tests needed to confirm the results and study the effect of pore fluid salt concentration
	From TDR	about 1GHz	(Wraith et al. 2001)	The thermodielectric model is persuasive; Correlations are good. Temperature control is needed, which is difficult to do in the field.
Hydraulic Conductivity	Electrical conductivity	< 1 MHz	(Arulanandan 1982; Arulmoli et al. 1985)	Theory is persuasive. Applicable for granular soils. Correlation is strong.
	Dielectric permittivity	1-150MHz	(Arulanandan 2003)	Reliability of the theory and experimental results need further study.
Residual Strength	Dielectric permittivity	1-150 MHz	(Arulanandan 2003)	Correlation from tests is strong. However, soil type used in tests is unclear. Validity unsure. No theory.
Compressibility $C_c$	Dielectric permittivity	1-150 MHz	(Arulanandan 1983)	Correlations from the tests are good and reasonable. No theory.
Swelling potential	Dielectric dispersion magnitude	1-150 MHz	(Basu 1973)	Correlations from tests are good and reasonable. No theory.
Time dependency of geomaterials properties	Dielectric permittivity and electrical conductivity	Various frequency	(Klein and Santamarina 2003)	Only qualitative analysis up to now.

### 2.4.1. Water Content and Dry Density

A typical soil is a three-phase mixture of air, water and solids. It is important to know the percentage of each phase in the mixture. Since the mass densities of water and solids are relatively constant ( $\rho_w \approx 1 \text{ g/cm}^3$  and  $\rho_s \approx 2.65 \text{ g/cm}^3$ ), the volumetric fraction of each phase can be determined if the gravimetric water content  $w$  and dry density  $\rho_d$  or the volumetric water content  $\theta$  and degree of saturation  $S_r$  are known. They are related as shown in Table 2.3.

Table 2.3 Determination of the volumetric fractions of the three phases in a soil

	From $w$ and $\rho_d$	From $\theta$ and $S_r$
$V_w$	$w \cdot \frac{\rho_d}{\rho_w}$	$\theta$
$V_s$	$\frac{\rho_d}{\rho_s}$	$1 - \frac{\theta}{S_r}$
$V_a$	$1 - w \cdot \frac{\rho_d}{\rho_w} - \frac{\rho_d}{\rho_s}$	$\frac{\theta}{S_r} - \theta$

\*Assume total volume  $V_t = 1$

In geotechnical engineering, measurements of  $w$  and  $\rho_d$  are frequently performed, because these two parameters can be readily measured in the lab if the excavated soil samples are available. However, it is not easy to quickly determinate these two parameters in the field. An alternative method is to determine the volumetric water content from electromagnetic measurements because the in-situ EM measurements can be very fast if time domain reflectometry (TDR) is used.

The successful use of TDR technology for soil water content measurement is largely attributed to Topp et al. (1980), who established a relation between soil volumetric water content  $\theta$  and the apparent dielectric constant  $\kappa_a$  from a TDR measurement:

$$\theta = 4.3 \times 10^{-6} \kappa_a^3 - 5.5 \times 10^{-4} \kappa_a^2 + 2.92 \times 10^{-2} \kappa_a - 5.3 \times 10^{-2} \quad [2.4]$$

where the apparent dielectric constant  $\kappa_a$  is calculated from the velocity at which the electromagnetic waves propagate in the soil. This velocity is actually determined by the equivalent dielectric permittivity of a soil. For coarse-grained soils with low pore fluid electrical conductivity, the equivalent dielectric permittivity is approximately equal to the real permittivity because the imaginary permittivity of these soils is small. The real permittivity a soil and its volumetric water content are closely related because water has a much higher real permittivity ( $\kappa_w' \approx 80$ ) than soil solids ( $\kappa_s' \approx 5$ ) and air ( $\kappa_a' \approx 1$ ). Thus, the measured real permittivity is primarily determined by the volumetric fraction of water.

The correlation [2.4] has been proven to be valid for saturated granular and low plasticity soils (Topp 1980). However, significant deviations were observed for organic soils and high plasticity soils (Dasberg and Hopmans 1992; Dirksen and Dasberg 1993; Dobson et al. 1985; Roth et al. 1992). The deviation can be due to two reasons: (1) the influence of the imaginary permittivity on the velocity of EM waves can no longer be ignored if the pore fluid DC electrical conductivity or surface conductance of a soil is high; (2) the empirical correlation established for saturated soils may not be valid when the degree of saturation  $S_r$  is much less than one, i.e., a deviation due to the density effect (Dirksen and Dasberg 1993; Jacobsen and Schjonning 1993).

To improve the precision of using the apparent dielectric permittivity for water content determination in compaction control, Siddiqui (1995) proposed a new correlation

by taking the effect of density into consideration and substituting the gravimetric water content  $w$  for the volumetric water content  $\theta$  for more direct application in compaction control.

$$\sqrt{\kappa_a} \frac{\rho_w}{\rho_d} = a + bw \quad [2.5]$$

where  $a$  and  $b$  are the fitting constants determined in the lab on soils to be compacted.

The procedure based on the above correlation has been incorporated into ASTM Standard (ASTM D6780-02) as a alternative approach to measure soil gravimetric water content and dry density. The ASTM procedure comprises two steps: (1) measure the apparent dielectric permittivity in the field using TDR; (2) excavate the soil being measured in the field, compact it in a mold and measure its total density and apparent dielectric permittivity again. From the apparent dielectric permittivity and total density, the gravimetric water content of the soil in the mold can be calculated. By assuming that the water content does not change during the process of soil excavation and compaction, the dry density in the field can be calculated using equation [2.5]. The disadvantage of this procedure is that the soil excavation is necessary in order to measure soil bulk density.

To avoid the inconvenience of soil excavation, the DC electrical conductivity has been used in combination with the apparent dielectric permittivity to simplify the ASTM procedure (Yu and Drnevich 2004) because the bulk soil electrical conductivity can also be readily measured using the TDR. The mechanism of the soil bulk electrical conductivity measurement using TDR will be introduced in Chapter 5.

The bulk electrical conductivity of a granular soil is primarily determined by the pore fluid electrical conductivity, which is similar to the contribution of the pore fluid to the apparent dielectric permittivity of the soil (Sihvola and Lindell 1990). Therefore, a

correlation similar to equation [2.5] was proposed by Feng et al. (1999) to relate the soil bulk electrical conductivity  $\sigma_b$  to the gravitational water content  $w$ :

$$\sqrt{\sigma_b} \frac{\rho_w}{\rho_d} = c + dw \quad [2.6]$$

where  $c$  and  $d$  are soil specific calibration constants.

Combining equations [2.5] and [2.6], Yu and Drnevich (2004) proposed a one-step method to determine the gravimetric water content  $w$  and dry density  $\gamma_d$  by simultaneously measuring apparent dielectric permittivity and bulk soil electrical conductivity (one-step method) using TDR.

$$\rho_d = \frac{d\sqrt{K_a} - b\sqrt{\sigma_b}}{ad - cb} \rho_w \quad [2.7]$$

$$w = \frac{c\sqrt{K_a} - a\sqrt{\sigma_b}}{b\sqrt{\sigma_b} - d\sqrt{K_a}} \quad [2.8]$$

The one-step procedure only requires a single TDR measurement in the field. It is an improvement over the ASTM Standard (D6780-02) procedure because no soil sampling is needed. Figure 2.3a is a comparison between the water contents determined by the one-step method and those determined by the oven-dry method on 14 different sands, two silts, seven different clays, one lime-stabilized soil and one low-density mixed waste. Figure 2.3b is a comparison between the TDR-measured dry densities and directly measured dry densities for these soils. These comparisons show that the one-step method has sufficient accuracy for geotechnical purposes. These good correlations also demonstrate that the electromagnetic waves can be a very promising tool for quantitatively determination of some engineering indexes if the relationships between the EM properties and engineering indexes can be fully understood. However, the one-step

procedure requires calibration of the fitting constants for each soil being tested at different pore fluid electrical conductivities, which is not practical for in-situ water content measurements of natural soils.

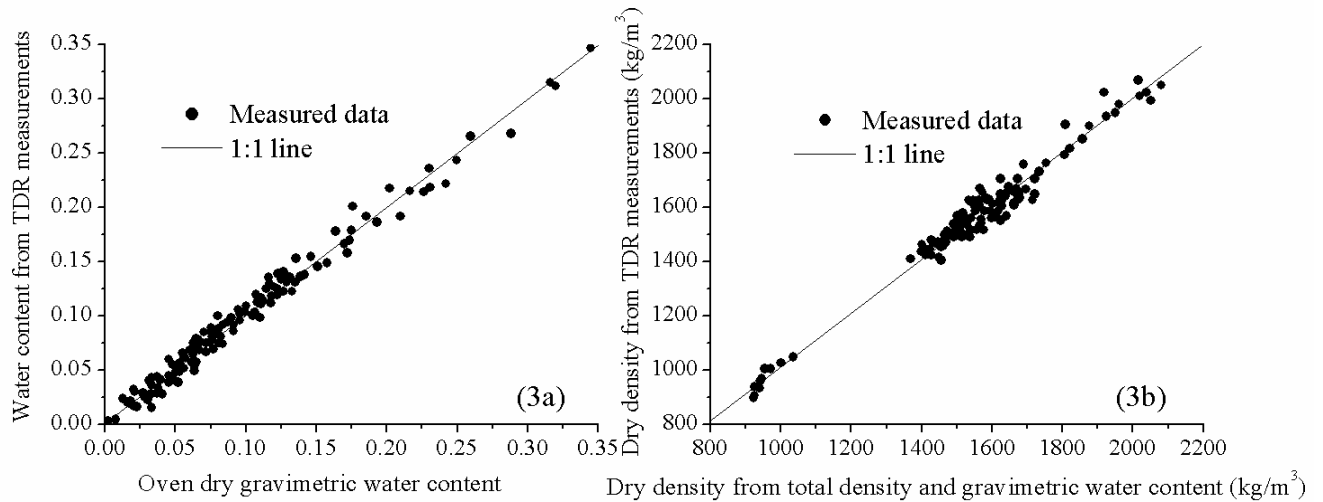


Figure 2.3 (a) Comparison of TDR-measured water contents with oven-dry water contents on 14 different sands, two silts, seven different clays, one lime-stabilized soil and one low-density mixed waste; (b) Comparison of TDR-measured dry density with directly measured dry density on the above soils (from Yu and Drnevich 2004)

### 2.4.2 Void Ratio and Anisotropy

The void ratio of a granular soil is usually related to its electrical properties through a formation factor. The formation factor  $F$  was firstly defined by Archie (1942) as the ratio between the electrical conductivity of the pore fluid  $\sigma_1$  and that of the sand-water mixture  $\sigma_m$  :

$$F = \frac{\sigma_1}{\sigma_m} \quad [2.9]$$

Dafalias and Arulanandan (1979a) redefined the formation factor by considering the effect of frequency on soil EM properties:

$$F_m = \frac{(\sigma_1 - \sigma_2) + j\omega(\kappa_1 - \kappa_2)\epsilon_0}{(\sigma_m - \sigma_2) + j\omega(\kappa_m - \kappa_2)\epsilon_0} \quad [2.10]$$

where  $\sigma_1$ ,  $\sigma_2$  and  $\sigma_m$  are the dc electrical conductivities of the pore fluid, solid particles and the mixture;  $\kappa_1$ ,  $\kappa_2$  and  $\kappa_m$  are the dielectric permittivities of the pore fluid, solid particles and the mixture, respectively.  $\omega$  is the angular frequency at which the formation factor is defined;  $\epsilon_0$  is the dielectric constant of the vacuum.

The formation factor thus defined is identical to:

$$F_m = \frac{\kappa_1^* - \kappa_2^*}{\kappa_m^* - \kappa_2^*} \quad [2.11]$$

where  $\kappa_1^*$ ,  $\kappa_2^*$  and  $\kappa_m^*$  are the equivalent dielectric permittivities of the pore fluid, soil particles and the mixture respectively.

At low frequency,  $F_m$  is reduced to  $(F_m)_0 = \frac{\sigma_1 - \sigma_2}{\sigma_m - \sigma_2}$  because the values of the imaginary components in equation [2.11] are much smaller than their corresponding real components. For granular soils, it can be further simplified to  $(F_m)_0 = \frac{\sigma_1}{\sigma_m}$  because the dc electrical conductivity of sand particles  $\sigma_2$  is almost zero. Therefore, at low frequencies, equation [2.11] is identical to the one defined by Archie (1942).

When the frequency is very high, Equation [2.11] can be reduced to  $(F_m)_\infty = \frac{\kappa_1 - \kappa_2}{\kappa_m - \kappa_2}$  because the real components in equation [2.11] become negligible compared with their corresponding imaginary components.



The formation factor is dependent on the direction of measurement if the soil is anisotropic. At low frequencies, where the influence of the dc electrical conductivity dominates, the formation factor in the vertical direction is:

$$(F_v)_0 = \frac{\sigma_1 - \sigma_2}{\sigma_v - \sigma_2} \quad [2.12]$$

Correspondingly, the formation factor in the horizontal direction is:

$$(F_h)_0 = \frac{\sigma_1 - \sigma_2}{\sigma_h - \sigma_2} \quad [2.13]$$

where  $\sigma_v$  and  $\sigma_h$  are the soil DC electrical conductivities measured in the vertical and horizontal directions.

For a transversely isotropic soil, the average formation factor at low frequencies  $\bar{F}_0$  is defined as:

$$\bar{F}_0 = \frac{(F_v)_0 + 2(F_h)_0}{3} \quad [2.14]$$

The average formation factor at high frequencies  $\bar{F}_\infty$  can be defined similarly by measuring the dielectric permittivities in the vertical and horizontal directions.

#### 2.4.2.1 Average void ratio of saturated soils

A theoretical relationship between the average formation factor  $\bar{F}_0$  from a DC electrical conductivity measurement and porosity  $n$  was developed by Dafalias and Arulanandan (1979b) for saturated uncemented granular soils based on the Maxwell-Fricke electromagnetic theory (Frick 1924):

$$\bar{F}_0 = n^{-\bar{J}} \quad [2.15]$$

where  $\bar{f}$  is the average shape factor, whose value is related the shape of the solid particles but independent of the orientation of these particles in the mixture.

$$\bar{f} = \frac{3S + 1}{6S(1 - S)} \quad [2.16]$$

The shape factor S of ellipsoidal particles with semiaxes a, b and c was derived by (Dafalias 1979):

For prolate spheroids ( $a > b = c$ ),

$$S = \frac{1}{2(1 - R^2)} \left[ \frac{R^2}{2\sqrt{1 - R^2}} \ln \frac{1 - \sqrt{1 - R^2}}{1 + \sqrt{1 - R^2}} + 1 \right], \quad (0 \leq R \leq 1) \quad [2.17]$$

For oblate spheroids ( $a < b = c$ ),

$$S = \frac{1}{2(R^2 - 1)} \left[ \frac{R^2}{\sqrt{R^2 - 1}} \tan^{-1} \sqrt{R^2 - 1} - 1 \right], \quad (R \geq 1) \quad [2.18]$$

where R is the axial ratio between the semiaxes  $R = b/a$ .

Equation [2.15] is identical to Archie's law (Archie 1942) in form. Thus the theory both validated Archie's law from the electromagnetic perspective and provided a means to investigate the influences of particle shapes on the DC electrical conductivity of granular soils. The theoretical relationships between the average formation factor and porosity are plotted in Figure 2.4 for prolate spheroids ( $R=0.01$ ), spheres ( $R=1$ ) and oblate spheroids ( $R=10$ ). It can be seen that the  $1/\bar{F}_0 - n$  correlation for prolate spheroids is close to that for spheres while the correlation for oblate spheroids deviates from that for spheres, indicating a large influence of the particle shape if the particles are flat.

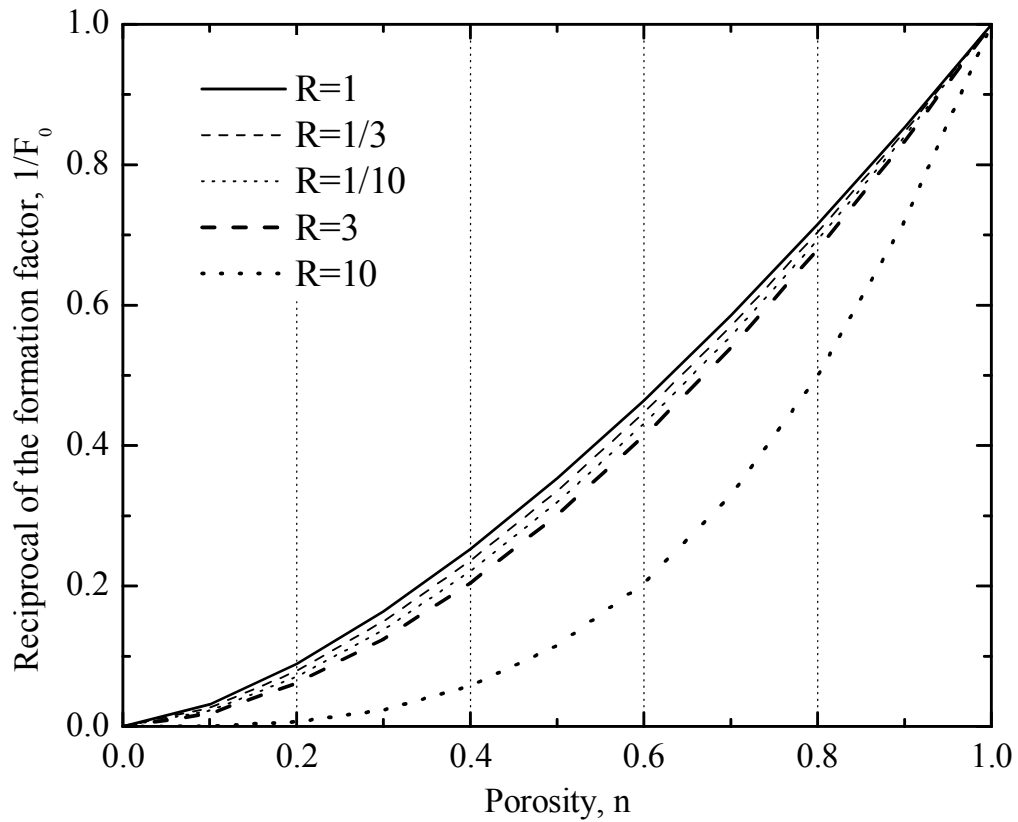


Figure 2.4 Correlation between porosity and average formation factor calculated from DC electrical conductivity

It is also possible to determine the porosity of a soil by measuring the average formation factor of a soil at high frequencies. According to Fernando et al. (1977), the average formation factor of a soil at high frequencies is related to its porosity by:

$$\bar{F}_\infty = 1 + \frac{1-n}{n} \left( \frac{3\kappa'_w}{2\kappa'_w + \kappa'_s} \right) \quad [2.19]$$

where  $\kappa'_w$  = real permittivity of free water at frequencies less than 1 GHz ( $\approx 79$  at a temperature of 20 °C).  $\kappa'_s$  = real permittivity of sand particles  $\approx 4.4$ .

The theoretical correlation between the porosity and the reciprocal of the average formation factor  $1/(\overline{F}_\infty)$  is shown in Figure 2.5. Also plotted are the experimental data for both sand and clay over the porosity range from 0.32 to 0.86, where the average formation factor was calculated from the measured real permittivity at 50 MHz.

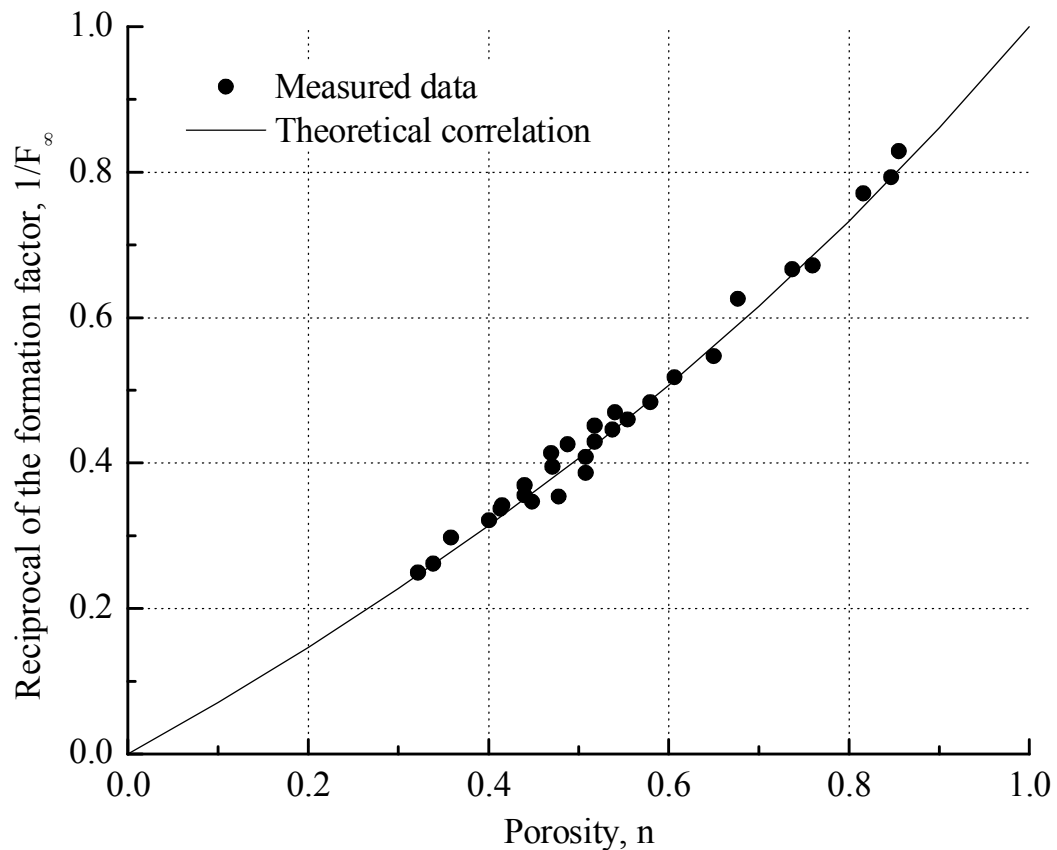


Figure 2.5 Correlation between porosity and the reciprocal of the formation factor calculated from the real permittivity at 50 MHz (data from Fernando, 1977)

Despite the fact that the theoretical correlation between the porosity and average formation factor was developed for granular soils, Figure 2.5 shows the correlation applies for a variety of soils including clay. Such a good correlation between the real permittivity and porosity for clay is surprising because the real permittivity of clay is affected by not only the porosity but also many other factors such as the specific surface

area, surface conductivity and pore fluid electrical conductivity. It will be shown in the next chapter that the correlation established for sand may not apply for clayey soils.

#### 2.4.2.2 Local void ratios

Sometimes, the distribution of local void ratio is more pertinent to the behavior of a soil than the average void ratio. For example, the volume change of a soil under drained conditions or the pore water pressure accumulation in undrained conditions can be dominated by the loosest or densest portion of the void distribution, and the hydraulic conductivity is governed by the interconnected larger pores (Frost 2000). Dong and Wang (2005) showed that the local void ratio can be obtained by measuring the local real permittivity using a slim form dielectric probe with an outside diameter of 2.2 mm. When water is tested, the range that can be detected by the slim form dielectric probe is approximately 2.5 mm.

Two correlations have been used to relate the measured real permittivity  $\kappa'_m$  to the porosity  $n$ :

(1) The Maxwell-Garnett (MG) mixing rule

$$n = 1 - \frac{(\kappa'_m - \kappa'_w)(\kappa'_s + 2\kappa'_w)}{(\kappa'_m + 2\kappa'_s)(\kappa'_s - \kappa'_w)} \quad [2.20]$$

where  $\kappa'_w$  is the real permittivity of free water at 1 GHz ( $\approx 79$  at 20 °C);  $\kappa'_s$  is the real permittivity of the solid particles ( $\approx 5$ );  $n$  is the porosity of the soil.

(2) The Lichtenecker empirical equation (Tinga 1973)

$$n = 1 - \frac{\text{Log}(k'_m) - \log(k'_w)}{\text{Log}(k'_s) - \log(k'_w)} \quad [2.21]$$

All parameters are defined previously.

Experiments on saturated sand and mica flakes showed that the mixing formula [2.20] satisfactorily estimated the porosity of the saturated sand but significantly underestimated the porosity of the mica flakes. In contrast, empirical equation [2.21] overestimated the porosity of the sand but gave a reasonable estimation for the porosity of the mica flakes. The Maxwell-Garnett mixing formula failed to correctly predict the porosity of the mica flakes because the mica flakes have a layered anisotropic structure, which severely deviates from the spherical inclusion assumption of the Maxwell-Garnett mixing formula. This effect of non-spherical particles and anisotropy on real permittivity is discussed in the next chapter.

#### 2.4.2.3 Anisotropy

The anisotropy of a granular soil can be evaluated from its DC electrical conductivities in different directions. Numerical analyses for the hydraulic flow through a medium with elliptical inclusions (Meegoda et al. 1989) have shown that the product of the intrinsic hydraulic permeabilities  $K$  in any mutually perpendicular directions  $\alpha$ ,  $\beta$ , and  $\gamma$  is approximately constant:

$$K_{avg}^3 = K_\alpha \cdot K_\beta \cdot K_\gamma \quad [2.22]$$

For a transversely isotropic medium where  $K_\beta = K_\gamma$ , an anisotropic factor A in the  $\alpha$  direction can be defined as:

$$A_\alpha = \left( \frac{K_\alpha}{K_{\alpha+90^\circ}} \right)^{2/3} \quad [2.23]$$

Due to the similarity of the hydraulic flow and the electrical flow through granular soils, Meegoda et al. (1989) suggested that this anisotropic factor can also be obtained by measuring the DC electrical conductivities in the vertical and horizontal directions.

$$A^e_v = \left( \frac{F_h}{F_v} \right)^{2/3} \quad [2.24]$$

$$A^e_h = \left( \frac{F_v}{F_h} \right)^{1/3} \quad [2.25]$$

where  $F_v$  and  $F_h$  are the formation factor in the vertical and horizontal directions as defined in equations [2.12] and [2.13].

For soils containing clay minerals, the clay surface conductance plays an important role in determining the soil bulk electrical conductivity and the simple analogue between the hydraulic flow and electrical current through the soil is no longer valid. As a result, the anisotropic factor as defined above may not be directly used for soils containing clay minerals.

#### 2.4.2.4 Small strain shear modulus

The small strain shear modulus of a soil is an important parameter for many geotechnical analyses including the earthquake ground response analysis, dynamic analysis of machine foundations and liquefaction potential assessment. The small strain

shear modulus is closely related to the effective confining pressure  $\sigma'_m$  and also affected by such factors as the void ratio, geological age of a deposit and cementation (Seed and Idriss 1970). The effects of all these factors can be expressed by a stiffness parameter  $K_{2_{\max}}$ , and the small strain shear modulus  $G_{\max}$  (Pa) can be expressed as:

$$G_{\max} = 1000 \cdot K_{2_{\max}} (\sigma'_m)^{1/2} \quad [2.26]$$

The value of  $K_{2_{\max}}$  ranges from 33 for loose sands to 70 for dense sands (Seed and Idriss).

A simple method for determining the small strain shear modulus of a soil is to measure its shear wave velocity  $V_s$  (m/s) because:

$$G_{\max} = \rho_t V_s^2 \quad [2.27]$$

where  $\rho_t$  is the total mass density of the soil ( $\text{kg/m}^3$ ).

If the total mass density of a soil and the effective confining pressure are known, the stiffness parameter  $K_{2_{\max}}$  can be calculated from the shear wave velocity by combining equations [2.26] and [2.27]. The  $K_{2_{\max}}$  calculated from the shear wave velocity was found to correlate well with a combination of electrical indexes (Arulmoli et al. 1985) as shown in Figure 2.6.



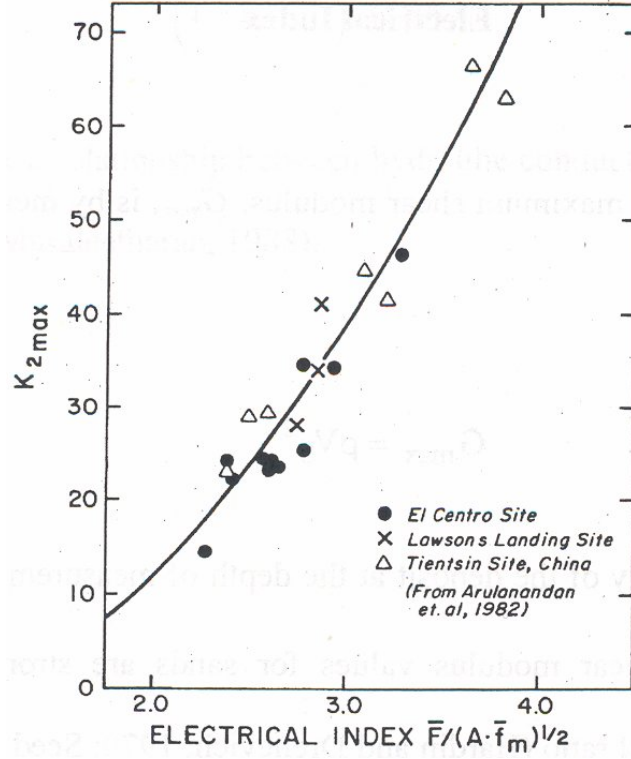


Figure 2.6 Correlation between the stiffness parameter and a combination of electrical indexes (from Arulmoli et al. 1985)

In the figure, the average formation factor  $\bar{F}$  is defined in equation [2.14]. The anisotropy index  $A$  is defined as:

$$A = \left( \frac{F_v}{F_h} \right)^{1/2} \quad [2.28]$$

where  $F_v$  and  $F_h$  are the formation factors in the vertical and horizontal directions.

The mean shape factor  $\bar{f}_m$  is defined as

$$\bar{f}_m = \frac{\bar{f}_{\max} + \bar{f}_{\min}}{2} \quad [2.29]$$

where  $\bar{f}_{\max}$  and  $\bar{f}_{\min}$  are the average shape factor  $\bar{f}$  at the maximum and minimum void ratios. Their values for a number of granular soils were measured by Arulmoli et al. (1985) as listed in Table 2.4.

Table 2.4 Average shape factors at maximum and minimum void ratios for granular soils

Soil type	$\bar{f}_{\max}$	$\bar{f}_{\min}$	$\bar{f}_m$	$(\bar{f}_{\max} - \bar{f}_{\min}) / \bar{f}_m$ (%)
Ottawa 'C-109'	1.4	1.32	1.36	5.6
Niigata Site	1.62	1.6	1.61	1.2
Reid Bedford	1.54	1.45	1.50	6
Lucite Balls	1.48	1.37	1.43	7.4
Monterey '0'	1.54	1.46	1.50	5.4
Sierra Diamond	1.60	1.51	1.56	5.8
Monterey '0/30'	1.53	1.45	1.49	5.2

The table shows the average shape factor does not change much with void ratio (standard deviation < 10%). If the shape factor  $\bar{f}$  is considered as a soil-specific constant, the average formation factor  $\bar{F}$  is uniquely determined by the porosity according to

equation [2.15] and the combination of the electrical indexes  $\frac{\bar{F}}{\sqrt{A \cdot \bar{f}_m}}$  is equivalent to

$\frac{1}{\sqrt{aA \cdot n^a}}$ , where  $a$  is a constant. Thus, the relationship between the stiffness parameter

$K_{2_{\max}}$  and the combination of electrical indexes essentially reflects that the stress-

normalized small strain shear modulus is governed by the porosity and affected by the

anisotropy. With increase of porosity and anisotropy, the stress-normalized small strain

shear modulus in the vertical direction decreases. However, the reason why the electrical indexes should be so combined is unclear.

#### 2.4.2.5 Liquefaction potential

Similar to the stress-normalized small strain shear modulus, Arulmoli et al. (1985) suggests that the liquefaction potential of an uncemented granular soil can also be empirically correlated to a combination of the average formation factor  $\bar{F}$ , anisotropy index  $A$  and mean shape factor  $\bar{f}_m$ . The correlation between the cyclic stress ratio required to initiate liquefaction in 10 cycles and the combination of electrical indexes  $A^3 / (\bar{F} \cdot \bar{f}_m)$  is shown in Figure 2.7.

As previously discussed for the small strain shear modulus, the average shape factor can be considered as a soil-specific constant. Then the combination of the electrical indexes in Figure 2.7 is equivalent to  $\frac{A^3 n^a}{a}$ , which reflects that the liquefaction resistance decreases with increasing porosity and anisotropy. This is consistent with the observation in Figure 2.6 because the small strain shear modulus is one of most important factors affecting the liquefaction resistance (Salgado et al. 2000). It should be noted that the effect of the anisotropy has been amplified in Figure 2.7, which means an increase in anisotropy may only slightly decrease the small strain shear modulus of a soil but significantly decrease the liquefaction resistance. The reason why electrical indexes should be combined in such a way as shown in Figure 2.7 is unclear.

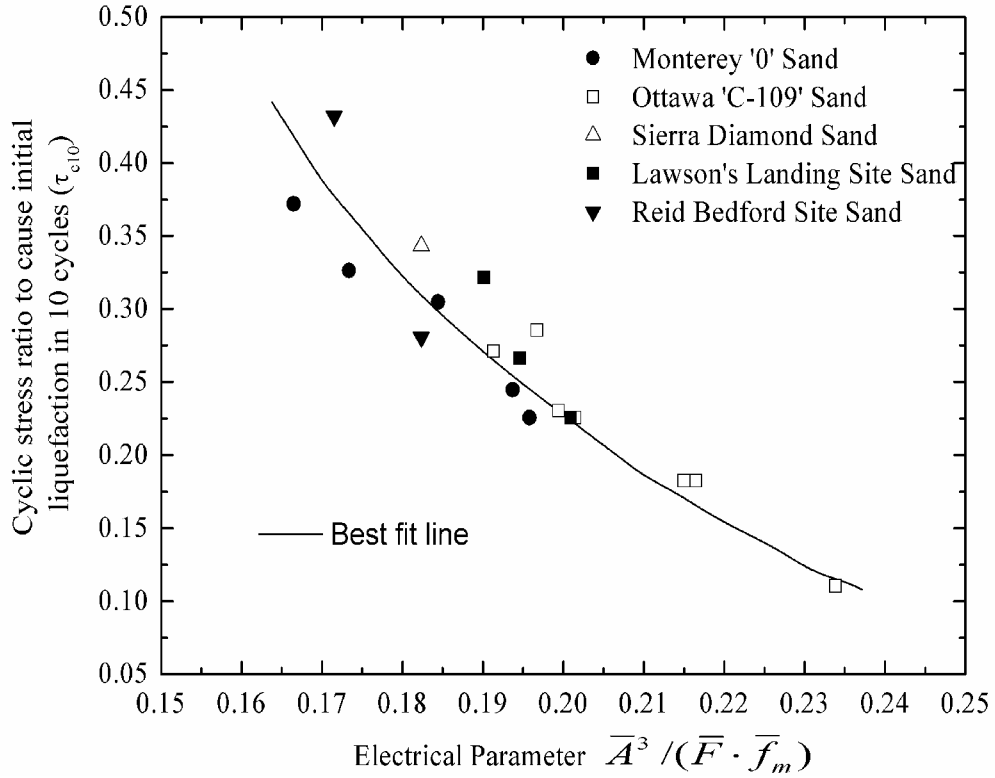


Figure 2.7 Laboratory correlation between cyclic stress ratio required to cause initial liquefaction in 10 cycles and a combination of electrical indexes (modified from Arulmoli 1985)

#### 2.4.2.6 Hydraulic conductivity from DC electrical conductivity

Several models have been established to relate the hydraulic conductivity of a soil to its internal geometry, characteristics of soil particles and properties of the pore fluids. Among them, the Kozeny-Carman equation (Carman 1937) is one of the most widely accepted models. The KC equation is expressed as:

$$K = k_h \left( \frac{\mu}{\gamma_p} \right) = \frac{1}{k_0 T^2 S_0^2} \left( \frac{e^3}{1+e} \right) \quad [2.30]$$

in which  $K$  = the intrinsic hydraulic permeability ( $m^2$ );  $k_h$  = the hydraulic conductivity ( $m/s$ );  $\mu$  = dynamic viscosity of the permeant ( $Ns/m^2$ ) =  $1.002 \times 10^{-3}$   $Ns/m^2$  for water at  $20^\circ C$ ;  $\gamma_p$  = the unit weight of the permeant ( $N/m^3$ ) =  $9.8 \times 10^3$   $N/m^3$  for water;  $k_0$  = the pore shape factor;  $T$  = the tortuosity factor;  $e$  = the global void ratio;  $S_0$  = the wetted surface per unit volume of particles ( $m^2/m^3$ ).  $S_0$  is related to the total specific surface area  $S_a$  ( $m^2/kg$ ) by:

$$S_0 = S_a \cdot \rho_s \quad [2.31]$$

where  $\rho_s$  is the mass density of the solid particles ( $kg/m^3$ ).

Generally,  $k_0 T^2 \approx 5 - 5.5$  is applicable for sands and most granular soils (Marcmullin and Muccini 1956). Thus, two critical parameters controlling the fluid flow are the void ratio and specific surface area.

For granular soils, the void ratio can be estimated from the average formation factor  $\bar{F}$  by measuring the DC electrical conductivity or real permittivity as discussed previously:

$$e = \frac{n}{1 - n} \quad [2.32]$$

$$n = \bar{F}^{-(1/\bar{f})} \quad [2.33]$$

The  $S_0$  of granular soils can be estimated from the gradation curve (Sanjeevan 1983):

$$S_0 = \frac{6 \left( \frac{W_1 - 0}{d_1} + \frac{W_2 - W_1}{d_2} + \frac{W_3 - W_2}{d_3} + \dots + \frac{100 - W_{n-1}}{d_n} \right)}{100} \quad [2.34]$$

where  $W_1, W_2, \dots$  etc., are the percentage passing and  $d_i$  is the average diameter between  $W_i$  and  $W_{i-1}$ .

Since  $k_0, T$  are relatively constant, a linear correlation should exist between the hydraulic conductivity and  $\frac{1}{S_0^2} \frac{\bar{F}^{-3/\bar{f}}}{(1 - \bar{F}^{-1/\bar{f}})^2}$ , which has been proven by Sanjeevan (1983)

from hydraulic conductivity tests on sands and silty sands as shown in Figure 2.8.

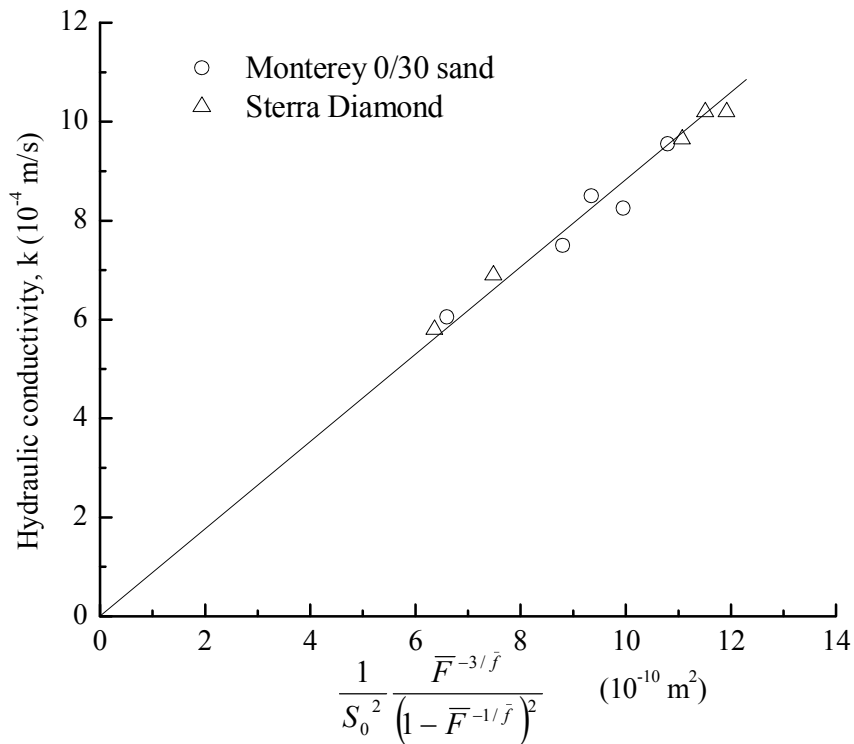


Figure 2.8 Correlation between the hydraulic permeability and electrical indexes (modified from Sanjeevan 1983)

Attempts to determine the hydraulic conductivity of clay from the electrical conductivity using the KC equation have been made (e.g. Sadek 1993, Arulanandan 2003) but were not very successful because it is difficult to determine the specific surface area of clay without disturbing its in-situ fabric. The research on the specific surface area determination using electromagnetic waves shown in Chapter 8 may provide a means to

overcome this difficulty and extend the application of the KC equation to determining the hydraulic conductivity of clay.

### **2.4.3 Specific Surface Area**

#### *2.4.3.1 From TDR-measured responses to thermal perturbation*

Water molecules close to soil surface are usually affected by surface forces arising from solid-phase surface atoms. These water molecules are called bound water molecules. Due to the high intensity of the forces acting upon them, the rotation of water molecules in an alternating electromagnetic field is hindered (Hallikainen et al. 1985). Therefore, bound water molecules have lower relaxation frequencies than free water molecules. At frequencies close to 1 GHz, the relaxation of bound water molecules has finished and their real permittivity drops to a value close to that of solid particles (~5) (Hilhorst 1998). In contrast, the relaxation of free water molecules has not started yet and the real permittivity of free water molecules is about 79 at 1 GHz. Since time domain reflectometry (TDR) measures the real permittivity of a soil at a frequency of about 1 GHz, only the amount of free water molecules is sensed by TDR. However, the thickness of the bound water layer decreases and the amount of free water molecules increases with increasing temperature. As a result, higher water content is sensed by TDR at higher temperatures.

Based on the above mechanics, Wraith (2001) developed a method to measure the soil specific surface area  $S_a$  from the temperature-dependent volume fraction of bound water  $\theta_{bw}(T)$ :

$$S_a = \theta_{bw}(T) / [x(T)\rho_b] \quad [2.35]$$

where  $x(T)$  = thickness of the bound water layer covering solid soil surfaces (m);  $\rho_b$  = dry density of the soil ( $\text{kg/m}^3$ )

By assuming that the bound water molecules are the water molecules with relaxation frequencies less than some cutoff frequency (for example, 1 GHz), the thickness of the bound water layer can be calculated (Wraith 2001):

$$x(T) = \frac{a}{-d + T \ln(m[f^*]T)} \quad [2.36]$$

in which  $m(f^*) = k / (8\pi^2 r^3 c f^*)$

where  $a$  is a coefficient derived by Low (1976) =  $1621 [\text{Å}\cdot\text{K}]$ ;  $d$  is a constant =  $2.047 \times 10^3$  [K];  $T$  is the absolute temperature;  $f^*$  is a certain cutoff frequency (1GHz);  $k$  is the Boltzmann constant;  $r$  is the radius of a water molecule  $\approx 3 \text{ Å}$  and  $c$  is a constant =  $9.5 \times 10^{-7}$  [Pa s].

From the measured responses of a soil to the thermal perturbation and the independently measured gravimetric water content and bulk soil density, the specific surface area can be determined. The specific surface area obtained from this method are in agreement with those measured by the ethylene glycol monoethyl ether (EGME) adsorption method as shown in figure 2.9. Generally, the TDR specific surface area is lower than the EGME, which indicates some intracluster specific surface area is not reflected by the TDR measurement. The problem with this method is that strict temperature control is required during the measurement and thus its application for in-situ soils is limited. Moreover, the measured data are quite scattered, indicating that the method is not very precise.



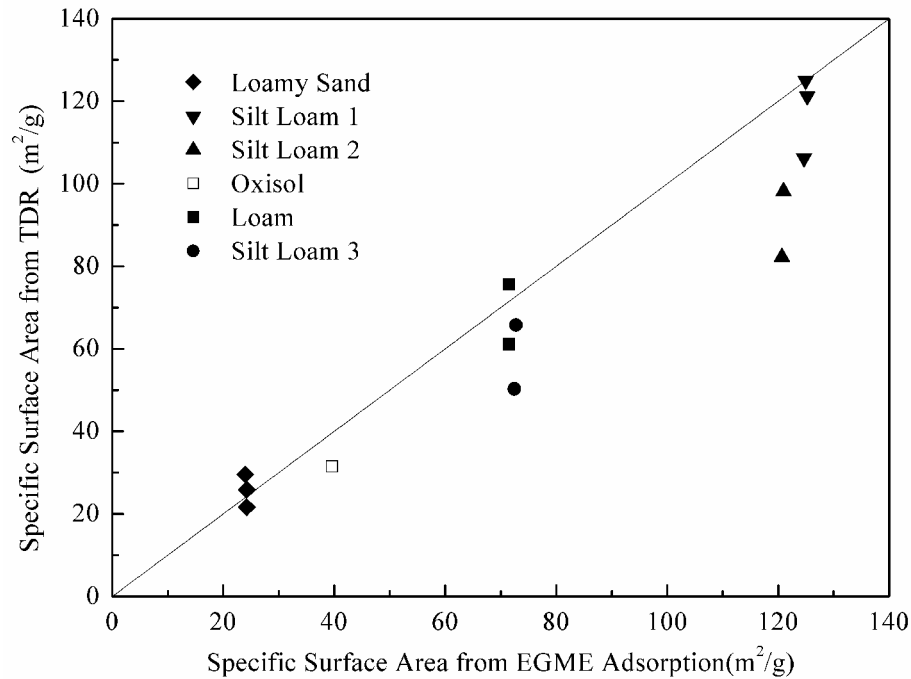


Figure 2.9 Comparison between the specific surface areas determined by the thermal disturbance method and those measured using the EGME adsorption method

#### 2.4.3.2 From dielectric dispersion magnitude

Many previous researches on the responses of soils to an electromagnetic field have shown that the real permittivity of soils containing clay minerals decreases with increasing frequency in the radio frequency range (e.g. Fernando et al.1977).

Linear correlations between the dielectric dispersion magnitude  $\Delta\kappa'$  over the 1 MHz and 100 MHz frequency range and specific surface area measured by the ethylene glycol monoethyl ether (EGME) adsorption method were observed by (Meegoda 1985) as shown in Figure 2.10.

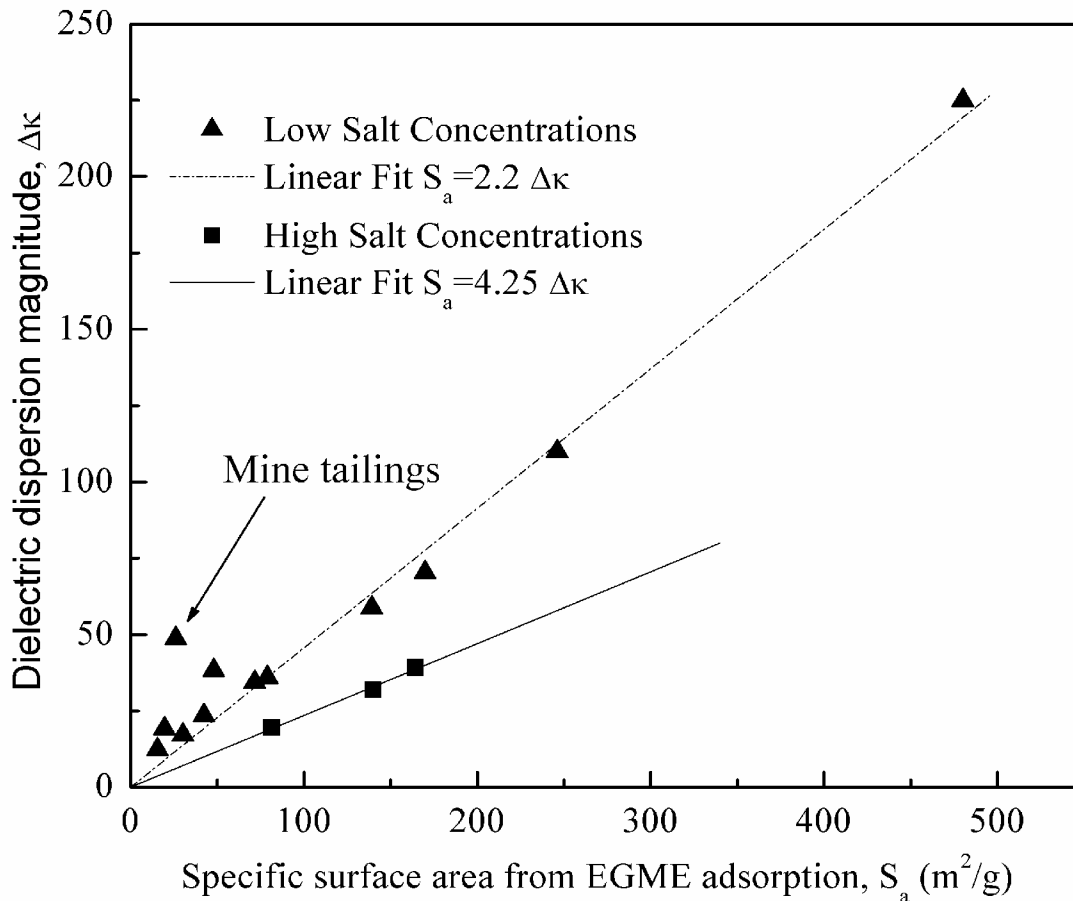


Figure 2.10 Dielectric dispersion magnitude from 1 MHz to 100 MHz and specific surface area from the ethylene glycol monoethyl ether adsorption method (data from Meegoda, 1985)

Interestingly, two correlations were given for different electrolyte salt concentrations, indicating that the pore fluid salt concentration has a large impact on the correlation. Unfortunately, the underlying mechanism why such good correlations exist is not fully understood and the influences of the pore fluid salt concentration could not be quantified.

Despite some uncertainties on the reliability of the correlation, the experimental results indicate that the dielectric dispersion measurement can be a promising approach for specific surface area measurement because the dielectric dispersion magnitude of a

soil can be readily measured. The reason why a good relationship should exist between the dielectric dispersion magnitude and specific surface area is explained in Chapter 3 and a discussion on how the pore fluid salt concentration and other factors affect the dielectric dispersion magnitude is presented in Chapter 4.

#### 2.4.3.3 *Strength (critical state friction angle)*

A linear correlation between the slope of the critical state line  $M$  and the dielectric dispersion magnitude  $\Delta\kappa$  from 1 MHz to 100 MHz was reported by Arulanandan (2003) as shown in Figure 2.11. The slope of the critical state line was obtained from triaxial tests and it is related to the critical state friction angle  $\phi_c$  by:

$$M = \frac{6 \sin \phi_c}{3 - \sin \phi_c} \quad [2.37]$$

The dielectric dispersion magnitude  $\Delta\kappa$  was measured on the same samples on which the critical state lines were determined. Since the type of soils and the detailed experimental processes were not described by Arulanandan (2003), the reliability of this correlation is uncertain.

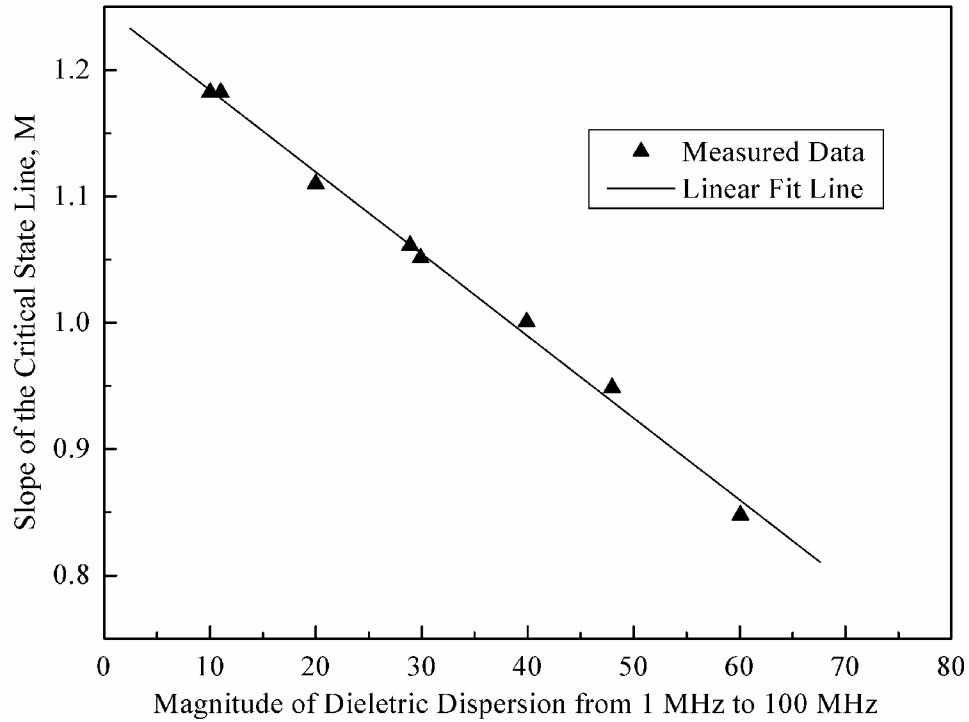


Figure 2.11 Slope of the critical state line in  $p'$ - $q$  space,  $M$ , versus the dielectric dispersion magnitude from 1 MHz to 100 MHz (From Arulanandan 2003)

#### 2.4.3.4 Compressibility

A correlation between the slope of the virgin consolidation line and the magnitude of dielectric dispersion from 1 MHz to 100 MHz was reported by Arulanandan et al. (1983) as shown in Figure 2.12. The Snow Cal is a soil with predominantly kaolinite minerals. In the mixtures of sand and montmorillonite, the weight percentages of montmorillonite are 3.3%, 5% and 10%, respectively. In the mixtures of silica flour and montmorillonite, the weight percentages of the montmorillonite are 3.3% and 5%.

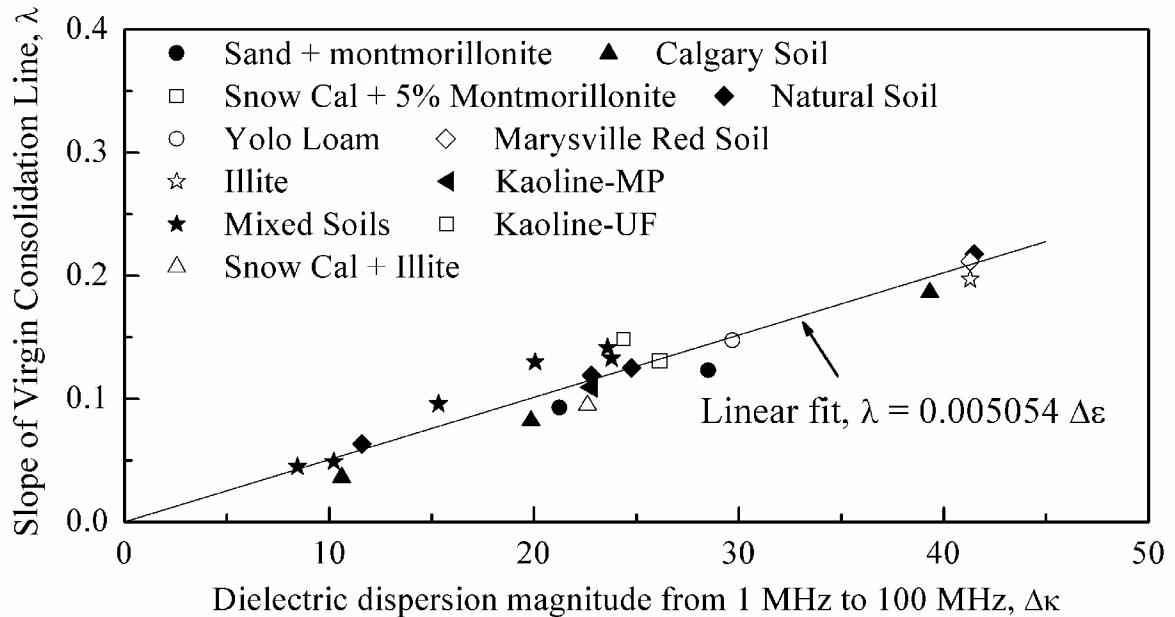


Figure 2.12 Slope of virgin consolidation,  $\lambda$ , versus dielectric dispersion magnitude over the 1 MHz to 100 MHz frequency range (from Arulanandan, et al. 1983)

The linear correlation  $\lambda = 0.005054\Delta\kappa'$  is applicable for clay minerals and for mixtures of clay and non-clay minerals whose maximum particle size is less than 0.01 mm (Arulanandan et al. 1983). With increase of the particle size of nonclay minerals, the mechanical interactions between larger particles prevail over the effects of clay minerals, which may lead to a lower compressibility than that predicted by the linear correlation shown in the figure.

#### 2.4.3.5. Swelling potential

The relationship between the swelling potential of a soil and its dielectric dispersion magnitude was studied by Basu and Arulanandan (1973). The relationship between the swelling potential and the dielectric dispersion magnitude from 1 MHz to 100 MHz is

shown in Figure 2.13. To measure the swelling potential of these soils, specimens were prepared by consolidating slurries of the soils under a pressure of 1 kg/cm<sup>2</sup>. Then, the cylindrical specimens of approximately 1 inch in height and 1.4 inch in diameter were allowed to dry at 65 °F and at 50 % relative humidity. Each dried sample was confined laterally and allowed to swell freely with no surcharge. Water was introduced by placing the soil on a porous stone that remained saturated with water during the test. The total swelling is expressed as a percentage of the initial height of the sample. It can be seen that the correlation between the swelling potential and the dielectric dispersion magnitude is fairly good if the Vermiculite is excluded.

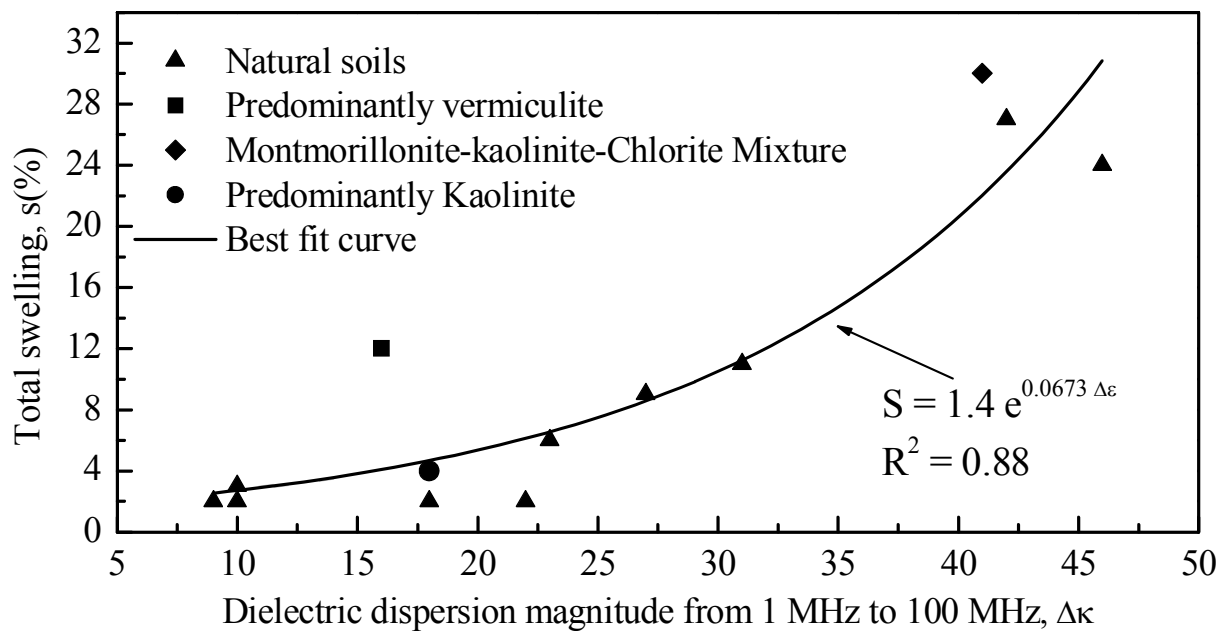


Figure 2.13 Total swelling potential versus dielectric dispersion magnitude from 1 MHz to 100 MHz (from Basu 1973)

#### *2.4.3.6 Comments on the dielectric dispersion magnitude and soil properties*

Figure 2.10 shows that good correlations exist between the total specific surface and the dielectric dispersion magnitude over the 1 MHz to 100 MHz frequency range. The dielectric dispersion magnitude, in turn, correlates well with the critical friction angle, compressibility and swelling potential as shown in Figures 2.11, 2.12 and 2.13, which means that the specific surface area and these engineering indexes are also highly correlated. All these correlations suggest that the specific surface area is an important parameter linking the electromagnetic properties and engineering properties of fine-grained soils. The importance of the specific surface area has long been recognized because of its critical role in determining many physiochemical and mechanical properties of fine-grained soils (Santamarina et al. 2002).

The above correlations also suggest that the dielectric dispersion magnitude has the potential to be a convenient and economical tool for determining the specific surface area and estimating such engineering indexes as the critical state friction angle, compressibility and swelling potential of fine-grained soils. However, at the same specific surface area, the dielectric dispersion magnitude of a soil can also be affected by other factors such as water content and pore fluid salt concentration. For example, the dielectric dispersion magnitude should be low when the water content is very low or very high. Therefore, the correlation between the dielectric dispersion magnitude and specific surface area can not be expected without considering the effects of water content and pore fluid salt concentration.

#### **2.4.4 Time Dependent Behavior**

Electromagnetic waves can be useful for studying the time-dependent soil behavior because they do not produce permanent residual effects or measurable perturbations on the tested materials (Santamarina et al. 2002). Applications have included the study of hydration processes of the cement paste (Christensen et al. 1994; McCarter and Afshar 1984) and sedimentation of the clay cement slurries (Fam and Santamarina 1996; Santamarina et al. 2002). During the entire physicochemical process, the changes in the dielectric permittivity and electrical conductivity of the tested sample can be monitored. Useful information about these processes can be acquired from the sample's responses to the EM waves at different phases. For example, the temporal variation in the electrical conductivity can be used as an indicator for different physicochemical stages and a decrease in the real permittivity at high frequencies indicates a reduction in the amount of free water. Most physicochemical processes, however, can only be qualitatively described because the relationships between the frequency-dependent electromagnetic properties of soils and their components and structure have not been fully understood. This study is necessary to better understand the responses of geomaterials to an EM field.

### **2.5 Conclusions**

A review of the applications of electromagnetic measurements for soil engineering property characterization and geo-process monitoring shows that:

(1) Both the DC electrical conductivity and high-frequency real permittivity have been successfully used to determine the porosity (volumetric water content) and



anisotropy of granular soils. Based on the measured porosity and anisotropic factor, the hydraulic conductivity, small strain shear modulus and liquefaction potential of granular soils can also be estimated.

(2) The application of electromagnetic measurements for estimating the engineering properties of fine grained soils is of high uncertainty. The main reason is that the relationship between the electromagnetic properties of fine-grained soils and their components and structure is not well understood and has not been quantified.

(3) The specific surface area seems to be a critical parameter to link the electromagnetic properties and engineering properties of fine-grained soils. Good correlations between the dielectric dispersion magnitude over the 1 MHz to 100 MHz frequency range and the specific surface area measured by the EGME adsorption method were observed. However, the correlation can be seriously affected by the pore fluid salt concentration and other factors. It is important to quantify the influences of these factors on the dielectric dispersion magnitude in order to establish a more reliable correlation.

In the following chapter, several theoretical and empirical correlations relating the electromagnetic properties of soils to their components and structure are reviewed. Their limitations are discussed. A new model is proposed through which various factors affecting the dielectric dispersion magnitude can be analyzed.